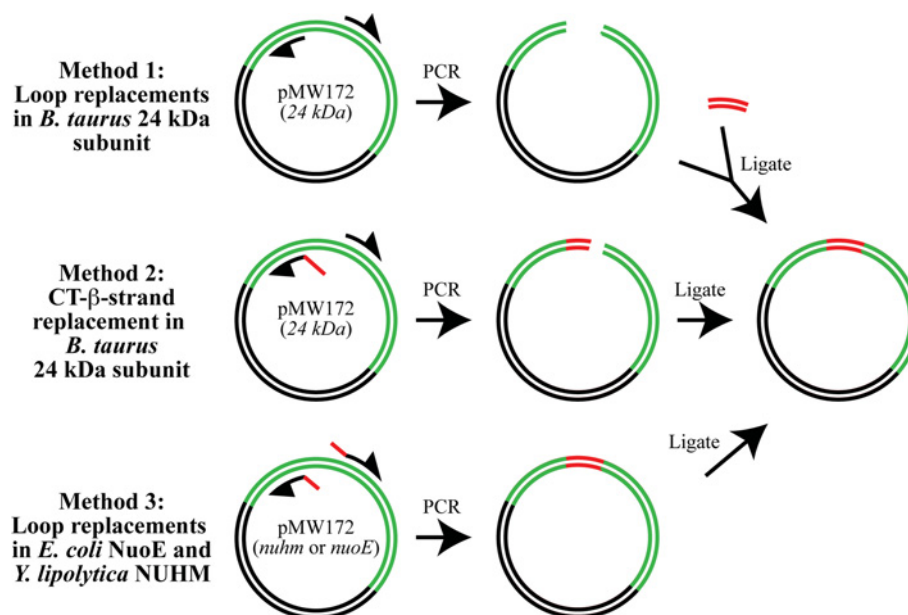


SUPPLEMENTARY ONLINE DATA

Investigating the function of [2Fe–2S] cluster N1a, the off-pathway cluster in complex I, by manipulating its reduction potential

James A. BIRRELL^{*}, Klaudia MORINA[†], Hannah R. BRIDGES^{*}, Thorsten FRIEDRICH[†] and Judy HIRST^{*1}^{*}MRC Mitochondrial Biology Unit, Wellcome Trust/MRC Building, Hills Road, Cambridge CB2 0XY, U.K., and [†]Institut für Biochemie, Albert-Ludwigs-Universität, Albertstrasse 21, 79104 Freiburg, Germany**Figure S1 Strategies for generating loop and CT-β strand replacements in the 24 kDa subunit plasmids**

The double circle (black and green) represents the pMW172 plasmid (black) containing the 24 kDa subunit protein-coding sequences (green). Black curved half-arrows represent the PCR primers used to generate linear double-stranded DNA fragments. The red lines represent the replacement sequence. The 24 kDa protein variants, with portions of the sequence replaced with homologous sequence from another species, were generated using three methods. (1) PCR was used to amplify a linear form of the parent plasmid without the region to be replaced (primers 13/14 and 19/20, Table S1), and then blunt-end ligation was used to insert the replacement sequence (primers 15/16 and 21/22, Table S1). (2) PCR was used to amplify a linear form of the parent plasmid that contained the replacement sequence (primers 25/26, Table S1), and then blunt-end ligation was used to circularize the plasmid. (3) PCR using primers (17/18 and 23/24, Table S1) that both contained half of the replacement sequence was used to amplify a linear form of the parent plasmid, and then blunt-end ligation was used to circularize the plasmid. Method 1 was used in earlier experiments, but produced false positives due to sequence insertion in the wrong direction. Methods 2 and 3 were used in later experiments; both methods were effective, but PCR was more successful with method 3 because the primers required are shorter and contain less mismatched sequence.

¹ To whom correspondence should be addressed (email jh@mrc-mbu.cam.ac.uk).

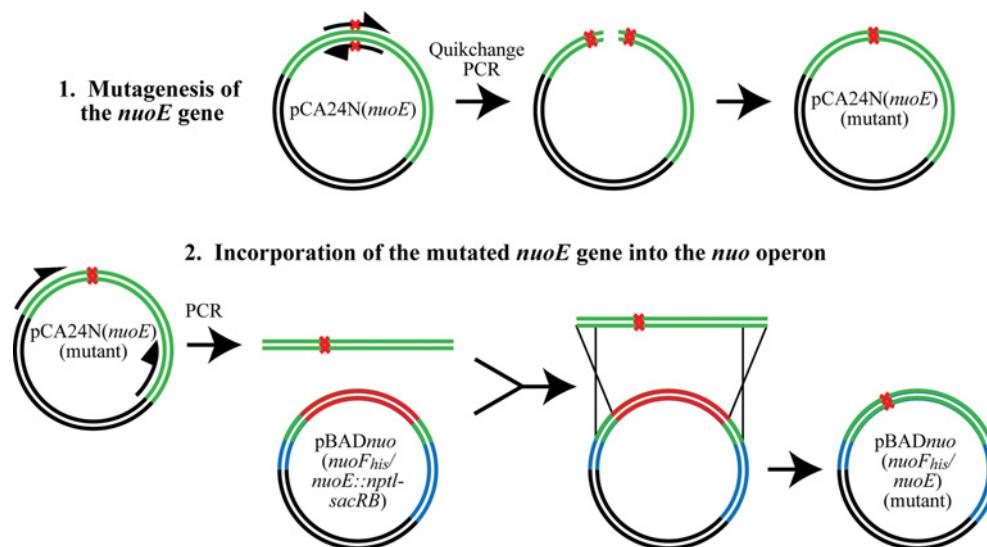


Figure S2 λ -Red-mediated recombineering strategy used to generate mutations in the 24 kDa subunit homologue (NuoE) in *E. coli* complex I

The green and black double circle [pCA24N(*nuoE*)] represents the plasmid containing the *nuoE* gene (green). The multicoloured double circle [pBAD*nuo*(*nuoF_{his}*/*nuoE*::*nptI-sacRB*)] represents the plasmid containing the whole *nuo* operon (blue), including the *nuoE* gene (green) which has been disrupted with the *nptI-sacRB* cartridge (red) from pUM24. (1) pCA24N(*nuoE*) was used for mutagenesis of the *nuoE* gene by QuikChange® (primers 37/38 and 39/40, Table S2) and the products were used to co-transform *E. coli* DH5 α ; the plasmid was amplified and purified. (2) PCR was used to amplify a linear fragment that included the mutated *nuoE* sequence (primers 41/42, Table S2), and this was used, in combination with pBAD*nuo*(*nuoF_{his}*/*nuoE*) to transform *E. coli* DH5 α Δ *nuo*/pKD46. Subsequently, site-specific recombination restored the complete *nuo* operon.

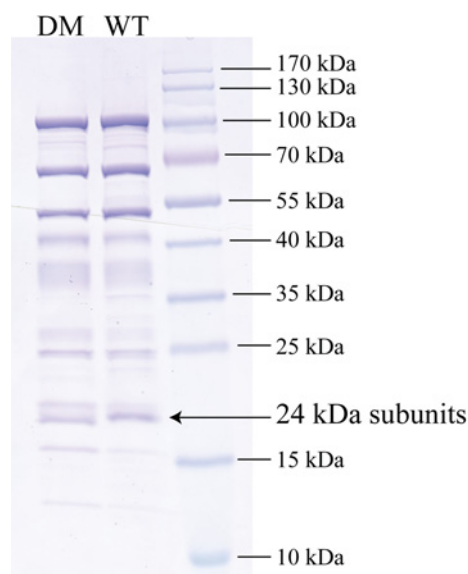


Figure S3 SDS/PAGE analyses of the wild-type and V96P/N142M (double mutant) variants of purified *E. coli* complex I

The sizes of a set of molecular-mass markers, and the positions of the 24 kDa subunits, are indicated. WT, wild-type; DM, double mutant (V96P/N142M). A total of 5 μ g of protein was loaded per lane.

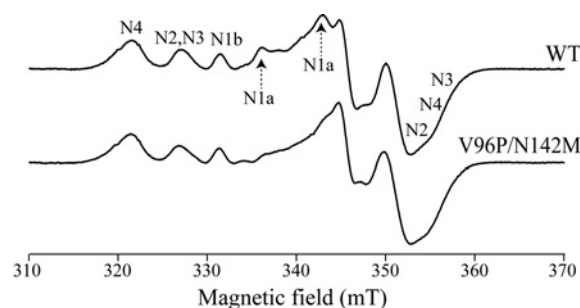


Figure S4 EPR spectra of the [4Fe-4S] clusters in the wild-type and V96P/N142M variants of *E. coli* complex I

Spectra were recorded at 12 K to focus on the complement of [4Fe-4S] clusters present, using 1 mW microwave power (see the legend to Figure 4 in the main paper for other experimental details). Key features from the clusters observed are marked (the [4Fe-4S] clusters are N2, N3 and N4). With the exception of the expected absence of signal N1a (present at low intensity at 12 K), the spectra of the wild-type (WT) and V96P/N142M variants are essentially indistinguishable.

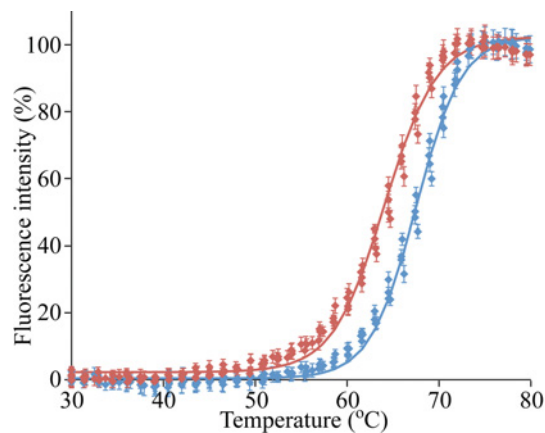


Figure S5 Thermal stability of the flavin site in the WT and V96P/N142M variant of *E. coli* complex I

The fluorescence of free flavin (the fluorescence of the complex I-bound flavin is quenched by the protein, and is not significant) was monitored using a real-time PCR machine as the temperature was increased. The data points are mean averages \pm S.E.M. ($n=4$). Blue, wild-type, $t_{1/2} = 67.1 \pm 0.1^\circ\text{C}$. Red, V96P/N142M variant, $t_{1/2} = 63.7 \pm 0.1^\circ\text{C}$. Conditions: protein concentration, $1 \text{ mg} \cdot \text{ml}^{-1}$, 20 mM Mops buffer, 150 mM NaCl, 10% glycerol, 0.05% dodecyl maltose neopentyl glycol, pH 7.5.

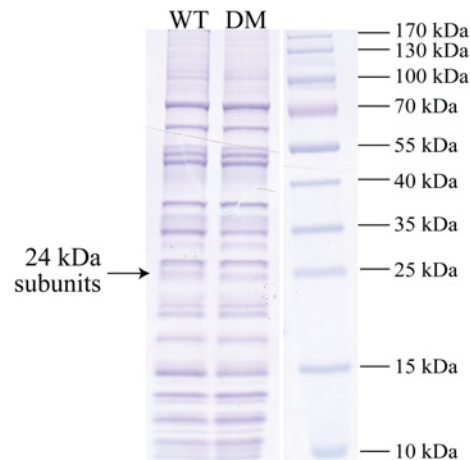


Figure S7 SDS/PAGE analyses of the wild-type and P103V/M149N variants of *Y. lipolytica* complex I

The sizes of a set of molecular-mass markers, and the positions of the 24 kDa subunits, are indicated. WT, wild-type; DM, double mutant (P103V/M149N). A total of $10 \mu\text{g}$ of protein was loaded per lane, and three lanes have been removed from between the lanes of interest and the marker lane.

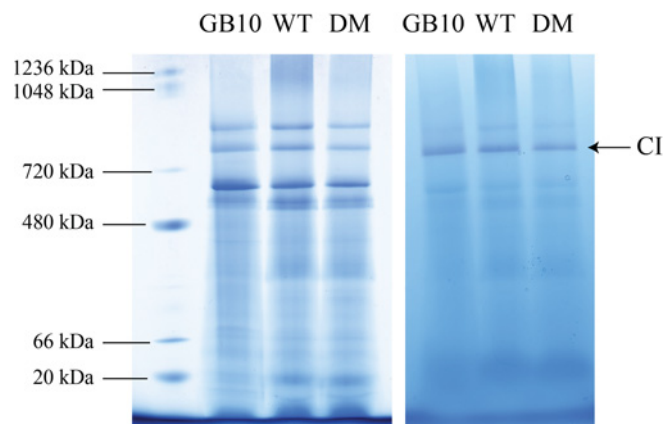


Figure S6 Blue native PAGE analysis of mitochondrial membranes from variants of *Y. lipolytica*

Membranes were solubilized using a detergent/protein ratio of 1.5:1 (protein concentration $10 \text{ mg} \cdot \text{ml}^{-1}$, *n*-dodecyl- β -*D*-maltoside). After centrifugation, $50 \mu\text{g}$ of solubilized proteins was loaded per lane. The gels were visualised using Coomassie Blue stain (left) or with the complex I in-gel activity assay (right). CI, complex I.

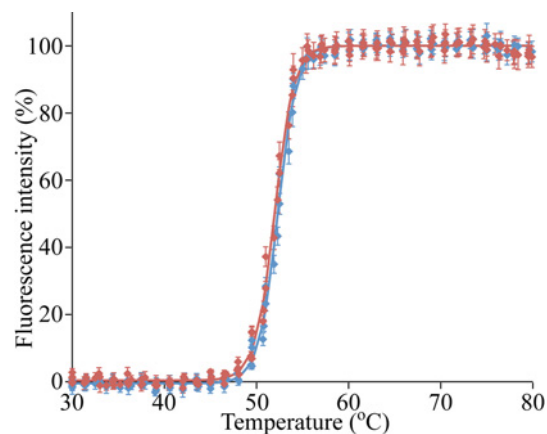


Figure S8 Thermal stability of the flavin site in the WT and P103V/M149N variants of *Y. lipolytica* complex I

The fluorescence of free flavin (the fluorescence of the complex I-bound flavin is quenched by the protein, and is not significant) was monitored using a real-time PCR machine as the temperature was increased. The data points are mean averages \pm S.E.M. ($n=4$). Blue, wild-type, $t_{1/2} = 52.2 \pm 0.1^\circ\text{C}$. Red, P103V/M149N variant, $t_{1/2} = 51.9 \pm 0.1^\circ\text{C}$. Conditions: protein concentration, $2 \text{ mg} \cdot \text{ml}^{-1}$, 20 mM Mops buffer, 150 mM NaCl, 10% glycerol and 0.05% dodecyl maltose neopentyl glycol, pH 7.5.

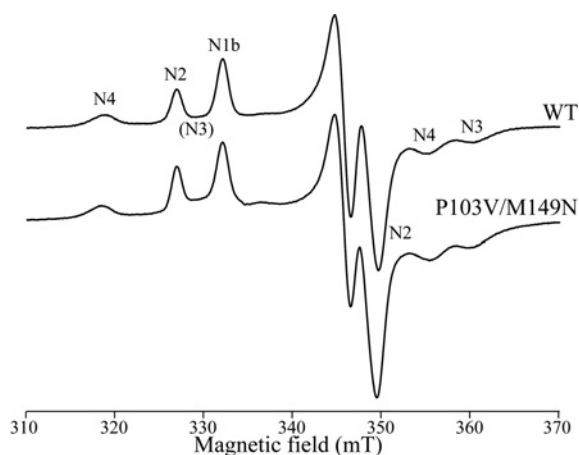


Figure S9 EPR spectra of the [4Fe-4S] clusters in the wild-type and P103V/M149N variant of *Y. lipolytica* complex I

Spectra were recorded at 12 K to focus on the complement of [4Fe-4S] clusters present, using 1 mW microwave power (see the legend to Figure 5 in the main paper for other experimental details). Key features from the clusters observed are marked (the [4Fe-4S] clusters are N2, N3 and N4; the g_z feature of N3 is broad in *Y. lipolytica*, and 'underneath' the signals from N2 and N1b). The spectra of the wild-type (WT) and P103V/M149N variants are essentially indistinguishable.

Table S1 Primers used to generate the mutants and sequence replacements of the 24 kDa subunits in the present study

The primers are named using the subunit to which they were applied (24 kDa for *B. taurus*, nuhm for *Y. lipolytica* and nuoE for *E. coli*) and the mutation/replacement that was made. The mutated positions/replacement sequence are underlined and in italics.

Primer number	Name	Sequence (5' → 3')
1	his-nuhm forward	AGACATATGCATCACCACCATCATCACACCCTCGGGCCCCCAGGG
2	his-nuhm reverse	TAGGAATTCATTAAATACCCCTCTGGAGG
3	24 kDa Q101R forward	GAGTCTGCACTACCACACCTTGC
4	24 kDa Q101R reverse	GAATGTGATACCTTCCAACAGGC
5	24 kDa D114N forward	AACAGCATACTGGAAGCCATTGAG
6	24 kDa D114N reverse	AGAGTTTCGGAGCATGCAAGGTGTGG
7	24 kDa E143C forward	TGTTGTTAGGGGCTGTGTAATGC
8	24 kDa E143C reverse	AACCTCTATAAGAGTGAAAAGTTTGTG
9	24 kDa E143Q forward	CAATGTTTAGGGGCTGTGTAATGC
10	24 kDa E143Q reverse	AACCTCTATAAGAGTGAAAAGTTTGTG
11	24 kDa N150K forward	AAAGCACAATGGTTCAAATAAATG
12	24 kDa N150K reverse	TACACAGGCCCTAAACATTCAAC
13	24 kDa Δ loop1 forward	TCTGACAGCATACTGGAA
14	24 kDa Δ loop1 reverse	GACTTGAATGTGATACTT
15	nuoE loop1 forward	<u>TGTGACAGCGTGGTCTGTCATATCAACGGT</u>
16	nuoE loop1 reverse	<u>ACCGTTGATATGACAGACCAGCGTGTGACA</u>
17	nuoE 24kDa loop1 forward	<u>ATGCTCCGAAACTATCAGGGTATTACGGCGGC</u>
18	nuoE 24kDa loop1 reverse	<u>GCAAGGTGGTAGTGCAATAACGGATCACATGG</u>
19	24 kDa Δ loop2 forward	GCACCAATGGTTCAAATA
20	24 kDa Δ loop2 reverse	TTCTATAAGAGTGAAAAG
21	nuoE loop2 forward	<u>ACTTGCTGCCTGGGAACTGTGATAAA</u>
22	nuoE loop2 reverse	<u>TTTATCACAGTTCCCAGGCAGCAAGT</u>
23	nuhm nuoE loop1 forward	GTCACATCAATGGCTCCGACGGTATCATGGAGG
24	nuhm nuoE loop1 reverse	AGACGACGCTGTACAGATCTGCAGATGGTACC
25	24 kDa nuoE CT- β forward	GACAACACTATGAGG
26	24 kDa nuoE CT- β reverse	<u>ATCGATCATCATGTTGGCCATTACACAGGCCCTAAAC</u>
26	24 kDa M153N forward	AAQTTCAAATAAATGAC
28	24 kDa M153N reverse	TGGTGCATTACACA
29	nuhm M149N forward	AACATGGCCATCAACGACG
30	nuhm M149N reverse	GGGGGCGTTGACACAGGC
31	nuoE N142M forward	ATGATGATGATCGATGAGGAC
32	nuoE N142M reverse	TGGCCCTTATCACAGTTCCC
33	nuhm P103V forward	GCTGTGACAGCTGTGGCTCCG
34	nuhm P103V reverse	GGTGGGTACAGATCTGC
35	nuoE V96P forward	<u>CCGTGTCATATCAACGGTTATCAGG</u>
36	nuoE V96P reverse	<u>CCTGATAACCGTTGATATGACA</u>

